

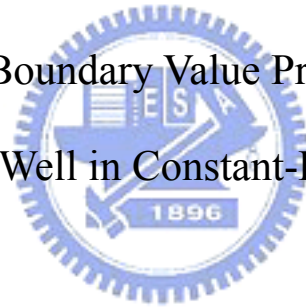
國立交通大學

環境工程研究所

博士論文

定水頭部分貫穿井混合邊界值問題之研究

Solutions for Mixed Boundary Value Problem Involving a Partially
Penetrating Well in Constant-Head-Test Aquifer



研究生：張雅琪

指導教授：葉弘德

中華民國九十八年四月

定水頭部分貫穿井混合邊界值問題之研究
Solutions for Mixed Boundary Value Problem Involving a
Partially Penetrating Well in Constant-Head-Test Aquifer

研究生：張雅琪

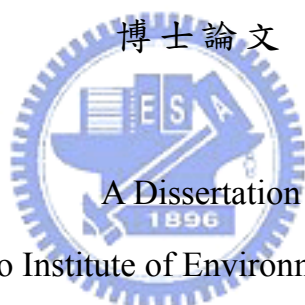
Student：Ya-Chi Chang

指導教授：葉弘德

Advisor：Hund-Der Yeh

國立交通大學

環境工程研究所



Submitted to Institute of Environmental Engineering

College of Engineering

National Chiao Tung University

for the Degree of

Doctor of Philosophy

in

Environmental Engineering

April 2009

Hsinchu, Taiwan

中華民國九十八年四月

定水頭部分貫穿井混合邊界值問題之研究

學生：張雅琪

指導教授：葉弘德

國立交通大學 環境工程研究所 博士班

中文摘要

含水層試驗通常為用來瞭解水層水文地質參數的重要工作。與水層試驗有關常用到的解析解，絕大多數是考慮井內的濾管(井篩)為全開的情況，即濾管貫穿整個水層的厚度。在濾管是全開的假設下，水層內的流況可視為水平流，在這種情況下，描述水層內水流的數學方程式不含垂直方向的分量，故較容易求得解析解。若考慮水層為部份貫穿，則數學上，定水頭試驗井會形成混合邊界，即在井緣同時存在兩種邊界，在井篩上為定水頭邊界，井篩外為不透水邊界。此混合邊界值問題，無法使用傳統的積分轉換方法求解，因而變得非常難解。在過去文獻中，對於此類混合邊界問題，皆將井緣的邊界條件作簡化以推求半解析解或解析解，然而這樣的解，計算得井緣附近的水位與流速場值，都會有數值誤差。

本研究利用 Laplace 及 finite Fourier cosine transform 將偏微分方程轉換成常微分方程式，接著代入井緣的邊界條件裡，形成一組 dual 或 triple series equations，最後解得方程式裡的未知係數，即可計算在侷限含水層中的洩降值。

關鍵字：地下水，含水層試驗，dual/triple series equations，侷限含水層，混合邊界值問題。

Solutions for Mixed Boundary Value Problem Involving a Partially Penetrating Well in Constant Head Tests Aquifer


Student: Ya-Chi Chang

Advisor: Dr. Hund-Der Yeh

Institute of Environmental Engineering

National Chiao Tung University

ABSTRACT

The logo of National Chiao Tung University is a circular emblem with a gear-like border. Inside the circle, there is a stylized building and the letters 'EISA' in a large font. Below the building, the year '1896' is inscribed. The logo is positioned behind the abstract text.

The mathematical model describing the aquifer response to a constant head test performed at a fully penetrating well can be easily solved by the conventional integral transform technique. The Dirichlet-type condition should be chosen as the boundary condition along the screen for such a test well. However, the boundary condition for a test well with partial penetration must be considered as a mixed-type condition. Generally, the Dirichlet condition is prescribed along the well screen and the Neumann type no-flow condition is specified over the unscreened part of the test well. The model for such a mixed boundary problem in a confined aquifer system of infinite radial extent and finite vertical extent is solved by the method of dual or triple series equations. This approach provides analytical results for the drawdown in the partially penetrating well and the well discharge

along the screen. The semi-analytical solutions are particularly useful for the practical applications from the computational point of view.

Key Words: groundwater, aquifer test, triple series equations, confined aquifer, mixed boundary value problem.



誌謝

本論文承蒙葉弘德教授細心指導與鼓勵，才得以順利完成，謹於此致上最誠摯的謝意。口試期間，台灣大學劉振宇教授、中國科技大學陳主惠教授、交通大學林振德教授，以及香港大學的焦剋剋教授對本文疏漏與謬誤上的指正，以及觀念上精闢的見解，使本論文更加充實完備，特於此一併致謝。

修業期間，葉弘德教授將專業知識傾囊相授，其認真的研究及生活態度，也令我受益良多。此外。感謝博士班時期的學長們，楊紹洋、王智澤、黃彥禎及林郁仲，他們在我研究上遇到問題或困難時，適時的給予經驗與指導，讓我在研究路途上更為順遂。也感謝實驗室學弟妹學業及生活上的相互扶持及幫助。

最後，最感謝的是我的家人，爸媽、大哥、大姐、二姐，因為他們的持續支持、鼓勵及愛護，才能使我安心的做研究。



TABLE OF CONTENTS

中文摘要	I
ABSTRACT	II
誌謝	IV
TABLE OF CONTENTS	V
LIST OF FIGURES	VI
NOMENCLATURE.....	VII
CHAPTER 1 INTRODUCTION.....	1
1.1 Background.....	1
1.2 Objectives	3
CHAPTER 2 LITERATURE REVIEW.....	5
CHAPTER 3 METHODOLOGY	8
3.1 Partially penetrating: screen extends from the top of the aquifer.....	8
3.2 Partially penetrating: arbitrary location of the well screen.....	12
CHAPTER 4 RESULTS AND DISCUSSION.....	14
4.1 Simplified solution	14
4.2 Numerical evaluations	14
4.3 Drawdown and well bore flux distribution.....	15
4.4 Effect of penetration ratio.....	17
CHAPTER 5 CONCLUSIONS	19
APPENDIX A	21
APPENDIX B	26
REFERENCES	30
VITA (個人簡歷).....	43
PUBLICATION LIST	44

LIST OF FIGURES

Figure 1. Schematic representation of a partially penetrating well with the screen extends from the top of the aquifer in a confined aquifer.....	33
Figure 2. Schematic representation of a partially penetrating well with arbitrary location of well screen in a confined aquifer.....	34
Figure 3. The drawdown distribution at dimensionless time $\tau = 1, 100, 10^4$ and $\tau = 10^6$ for various ρ	35
Figure 4. The distribution of flux along the well screen at different dimensionless time.....	37
Figure 5. The spatial drawdown contours at dimensionless time $\tau = 100, 10^3$ and $\tau = 10^4$	38
Figure 6. The spatial drawdown contours at dimensionless time $\tau = 10^5$ for various α^2 ...	39
Figure 7. The spatial drawdown contours at dimensionless time $\tau = 10^6$ for different screen location with $\beta = 50$. ($\xi_1 = 12.5$ and $\xi_2 = 37.5$; $\xi_1 = 25$ and $\xi_2 = 50$).....	40
Figure 8. The spatial drawdown contours as at dimensionless time $\tau = 10^7$ for $\xi_1 = 100$ and $\xi_2 = 150$	41
Figure 9. The influence of the penetration ratio on the flux.....	42

NOMENCLATURE

b	: thickness of aquifer (L)
d_1	: depth to bottom of the well screen (L)
d_2	: depth to top of the well screen (L)
$H(n,p)$: $K_1(\lambda_n)/K_0(\lambda_n)$
K_r	: radial hydraulic conductivity (LT^{-1})
K_z	: vertical hydraulic conductivity (LT^{-1})
$K_0(\cdot)$: modified Bessel function of the second kind of zero order
$K_1(\cdot)$: modified Bessel function of the second kind of first order
K_r	: horizontal hydraulic conductivity of unconfined aquifer
K_z	: vertical hydraulic conductivity of unconfined aquifer
l	: length of screen (L)
n	: finite Fourier cosine transform parameter of ξ
p	: Laplace transform parameter of τ
$P_n(\cos u)$: associated Legendre function
$\bar{q}^*(1, \xi, p)$: dimensionless well bore flux in Laplace domain
$\bar{Q}^*(p)$: dimensionless well discharge in Laplace domain
r	: radial distance (L)
r_w	: well bore radius (L)
s_w	: constant drawdown prescribed at the well (L)
$s(r, z, t)$: transient drawdown (L)
$s^*(\rho, \xi, \tau)$: dimensionless drawdown
$\bar{s}^*(\rho, \xi, \tau)$: dimensionless drawdown in Laplace domain
$\hat{s}^*(\rho, \xi, \tau)$: dimensionless drawdown in Laplace and Fourier domain

S_s	: specific storage coefficient (L^{-1})
t	: time (T)
z	: vertical distance (L)
α^2	: K_r / K_z , anisotropy ratio
β	: b / r_w , dimensionless aquifer thickness
λ	: l / r_w , dimensionless screen length
λ_n	: $\sqrt{(n\pi\alpha / \beta)^2 + p}$
η	: $n\pi / \beta$
μ_1	: $\xi_1\pi / \beta$
μ_2	: $\pi(1 - \xi_2 / \beta)$
ξ	: z / r_w , dimensionless vertical distance
ξ_1	: d_1 / r_w
ξ_2	: d_2 / r_w
ρ	: r / r_w , dimensionless radial distance
τ	: $K_r t / S_s r_w^2$, dimensionless time
ω	: l / b , partial penetration ratio
ψ_0	: $K_0(\sqrt{p\rho}) / K_0(\sqrt{p})$



CHAPTER 1 INTRODUCTION

1.1 Background

Hydraulic parameters, e.g., hydraulic conductivity, specific storage and leakage factor, are important for characterizing the aquifer and quantifying groundwater resources. Two typical pumping tests (i.e. constant-head and constant-rate pumping tests) are widely conducted by the hydrogeologists to determine the hydraulic parameters of the aquifer. In a constant-rate test, the well is pumped for a significant length of time at a constant rate and at least one observation is used to obtain the drawdown data. However, the pumped well may be overdrawn if the aquifer has low permeability. Therefore, the constant-head test is generally employed in this circumstance. During the test, the hydraulic head at the well is kept constant throughout the test period and the transient flow rate across the wellbore is measured at the same time. Rice [1998] mentioned that there are some merits in constant-head tests. In recent years, owing to the numerous important issues in the low-permeability aquifers, there has been an increasing interest in the study of constant-head tests. Jones et al. [1992] and Jones [1993] discussed the practicality of constant-head tests on wells completed in low-conductivity glacial till deposits. Mishra and Guyonnet [1992] indicated that the operational benefit of constant-head tests in situations where the total available drawdown is limited by well construction and aquifer characteristics. They

developed a method for analyzing observation-well response to constant-head test. For other environmental applications, light nonaqueous phase liquids (LNAPL) are typically recovered by wells held at constant drawdown [Murdoch and Franco, 1994]. The strategy for the contaminated site is to hold a slight drawdown and remove LNAPL as it accumulates in the well.

The wellbore storage plays an important role for estimating aquifer parameters in constant-rate tests. However, the effect of wellbore storage can be neglected for constant-head tests if the aquifer has low-conductivity and the radius of well is small.

Some aquifers are so thick that it is not justified to install a fully penetrating well. The pumping test has to be performed in a partially penetrating well instead of fully penetrating well. For example, the suggested length of screen is 6 m and the screen should be 1 m and 5 m below the water table at least for flood and dry seasons, respectively, for unconfined aquifers in Taiwan. For confined aquifer, the location of the screen is adapted for the purpose of the well. In addition, the partially penetrating well could be used in a pumping test to evaluate the hydrologic parameter in heterogeneous aquifers. Therefore, the issues involving partially penetrating well are studied in literatures [e.g., Cassiani and Kabala, 1998; Cassiani et al., 1999; Yang and Yeh, 2005].

The drawdown data may be influenced by the well skin effect produced by well construction. If the well skin effect is considered in the model, a more appropriate

description for such an aquifer system should treat the skin zone as a different formation zone instead of using a skin factor. Thus, the aquifer system naturally becomes a two-zone formation [see, e.g., Yang and Yeh, 2002; Yeh et al., 2003; Yang and Yeh, 2005; Yeh and Yang, 2006]. If the well skin effect is negligible in the model, the well loss can be ignored. The fully penetrating well can be simulated as a Dirichlet (also called the first type) boundary condition, and the relative models can be solved by the conventional integral transform techniques [Hantush, 1964]. For partially penetrating well, the Dirichlet boundary condition is suited to describe the drawdown along the well screen and the Neuman (second type) boundary condition is specified along the casing. Thus, the boundary condition along the well face in the partially penetrating well is a mixed type condition. The term “mixed-type” boundary condition is used to distinguish this boundary condition from the “uniform” Dirichlet and Neuman boundary condition or a combination of Dirichlet and Neuman boundary conditions.

1.2 Objectives

The purpose of this study is to develop a new solution to a constant head test performed in a partially penetrating well for arbitrary location of the well screen in an aquifer of finite thickness in depth. The study is based on the following assumptions: (1) The aquifer is homogeneous, infinite extent, and with a constant thickness; (2) the well has a finite radius; (3)

the initial head is constant and uniform throughout the whole aquifer; (4) the well loss is not considered in the system. Under these assumptions, this study will further compare the new solution to the existing solutions.



CHAPTER 2 LITERATURE REVIEW

Mixed boundary conditions are widely used to describe many boundary value problems of mathematical physics. Such problems arise in potential theory and its numerous applications to engineering, fracture mechanics, heat conduction, and many others. Only limited analytical solutions to mixed boundary problems (MBPs) in the field of well hydraulics have been found so far by special solution techniques including the dual integral/series equation [Sneddon, 1966], Weiner-Hopf technique [Noble, 1958], and Green's function [Huang and Chang, 1984]. Most of the solutions to MBPs have been obtained numerically or by approximate methods such as asymptotic analysis or perturbation techniques. Yedder et al. [1994] studied the steady heat conduction in a square plate with mixed boundary condition on a straight boundary using finite difference and control volume methods. They overcame the difficulties encountered in singular cases and discussed the convergence criteria used in the numerical treatment of these problems. Bassain et al. [1987] indicated that under certain circumstances, the mixed condition gives rise to singular behavior which cannot be adequately treated by numerical means alone. They discussed the implications of the singular behavior due to the mixed boundary condition of the adiabatic-isothermal type in the mathematical modeling heat transfer phenomena. Wilkinson and Hammond [1990] described a perturbation method to solve the MBPs in pressure

transient testing and obtained good results in a variety of well test problems of this type.

For the mathematical model under the mixed boundary condition in a confined aquifer of semi-infinite thickness, Cassiani and Kabala [1998] used the dual integral equation method to develop a Laplace domain solution that account for the effect of wellbore storage, infinitesimal skin, aquifer anisotropy and infinite aquifer thickness under constant-rate tests. Cassiani et al. [1999] further used the same method to develop the solutions in Laplace domain suited for constant head pumping tests and double packer tests that treated as the MBPs. Selim and Kirkham [1974] used the Gram-Schmidt orthonormalization method to develop a steady state solution in a confined aquifer of finite horizontal extent. Similar problems under the mixed boundary conditions also arise in the field of heat conduction. Among others, Huang [1985] used the Weiner-Hopf technique to develop a solution in a semi-infinite slab and Huang and Chang [1984] combined the Green's function with conformal mapping to develop the solution in an elliptic disk. The literatures listed above are under the assumption that the domain which the mixed boundary condition occurs is infinite. In reality, the thickness of aquifer is generally finite. Since the solutions in Cassiani and Kabala [1998] and Cassiani et al. [1999] are based on the infinite aquifer thickness assumption, they are only appropriate for the early time condition when the pressure change caused by the constant-head pumping has not reached the bottom of the aquifer or for the special condition where the screen length is significantly shorter than the aquifer thickness.

Chang and Chen [2002] removed such constraints by assuming finite aquifer thickness and treated the well skin effect as a skin factor. They also treated the boundary along the well screen as a Cauchy (third type) boundary condition and replaced the mixed boundary by homogeneous Neumann boundary. They considered the wellbore flux entering through the well screen as unknown and discretized the screen length into M segments. Thus, the discretization approach to deal with mixed boundary is numerical and their solution may be inaccurate if an improper choice of M is made. In other words, only when M approaches infinity, the solution can exactly represent the drawdown distribution in the problem domain.



CHAPTER 3 METHODOLOGY

3.1 Partially penetrating: screen extends from the top of the aquifer

The water level is held as a constant at a preselected depth while precisely measuring flow rate changes when conducting a constant-head test. Figure 1 shows a partially penetrating well in a confined aquifer of finite extent with a thickness of b under a constant-head test. The drawdown at the distance r from the well and the distance z from the bottom of the aquifer at time t is denoted as $s(r, z, t)$. The well screen extends from the top of the aquifer ($z = b$) to $z = d_1$ with a length of l . The hydraulic parameters of the aquifer are horizontal hydraulic conductivity K_r , vertical hydraulic conductivity K_z , and specific storage S_s . Since the flow velocities are so low and the pressure exerted by the atmosphere is more or less constant at a site in groundwater situations the velocity energy and the pressure are not taken into consideration in this study. Therefore, the governing equation for the drawdown can be written as [Yang et al., 2006]

$$K_r \left(\frac{\partial^2 s}{\partial r^2} + \frac{1}{r} \frac{\partial s}{\partial r} \right) + K_z \frac{\partial^2 s}{\partial z^2} = S_s \frac{\partial s}{\partial t} \quad (1)$$

Assuming that there is no flow toward to the bottom of the well, consequently a Dirichlet boundary condition for a fixed drawdown specified along the well screen is:

$$s(r_w, z, t) = s_w \quad d_1 \leq z \leq b \quad (2a)$$

A Neumann boundary condition of zero flux is specified as:

$$\left. \frac{\partial s}{\partial r} \right|_{r=r_w} = 0 \quad 0 \leq z \leq d_1 \quad (2b)$$

Moreover, the initial condition and other boundary conditions are:

$$s(r, z, 0) = 0 \quad (3)$$

$$s(\infty, z, t) = 0 \quad (4)$$

and

$$\frac{\partial s}{\partial z} = 0, \quad z = 0, z = b \quad (5)$$

Equation (1) may be expressed in dimensionless terms as:

$$\frac{\partial^2 s^*}{\partial \rho^2} + \frac{1}{\rho} \frac{\partial s^*}{\partial \rho} + \alpha^2 \frac{\partial^2 s^*}{\partial \xi^2} = \frac{\partial s^*}{\partial \tau} \quad (6)$$

subject to the boundary and initial conditions written in dimensionless terms as

$$s^*(\rho, \xi, \tau = 0) = 0 \quad (7)$$

$$s^*(\rho = \infty, \xi, \tau) = 0 \quad (8)$$

$$s^*(\rho = 1, \xi, \tau) = 1, \quad \xi_1 \leq \xi \leq \beta \quad (9a)$$

$$\left. \frac{\partial s^*}{\partial \rho} \right|_{\rho=1} = 0, \quad 0 \leq \xi \leq \xi_1 \quad (9b)$$

$$\frac{\partial s^*}{\partial \xi} = 0, \quad \xi = 0, \xi = \beta \quad (10)$$

where $s^* = s/s_w$ is the dimensionless drawdown, $\tau = tK_r/(S_s r_w^2)$ is the dimensionless time,

$\alpha^2 = K_z/K_r$ is the anisotropy ratio of the aquifer, $\beta = b/r_w$ is the dimensionless aquifer

thickness, $\rho = r/r_w$ and $\xi = z/r_w$ are dimensionless spatial coordinates, $\xi_1 = d_1/r_w$ is the

dimensionless depth at the bottom of the well screen. Note that Eqs. (6) - (10) constitute a

mixed-type boundary value problem.

The detailed development for the solution of Eq. (6) with Eqs. (7) – (10) using dual series equation and perturbation method is given in Appendix A. The solution for the drawdown in Laplace domain can be written as:

$$\bar{s}^*(\rho, \xi, p) = \frac{1}{2}B(0, p)\psi_0 + \sum_{n=1}^{\infty} B(n, p)\psi_n \cos(\eta\xi) \quad (11)$$

with $\eta = (n\pi)/\beta$, $\psi_0 = K_0(\sqrt{p\rho})/K_0(\sqrt{p})$ and $\psi_n = K_0(\lambda_n\rho)/K_0(\lambda_n)$. The coefficients in Eq. (11) can be calculated by the following equations

$$B_0 = \left(1 + \sqrt{p}H_0\Omega_1(\mu_1)\right)^{-1} \cdot \left[\frac{4}{p\pi}\Omega_3(\mu_1) + \frac{2}{p}(1 - \mu_1) + \sum_{k=1}^{\infty} \frac{2}{k} I_k C_k \Omega_2(\mu_1, k) \right] \quad (12)$$

and

$$B_n = \sum_{k=1}^{\infty} \frac{1}{k} I_k B_k \left[\Omega_2(\mu_1, k) \cdot f_2(n, \mu_1) - \int_0^{\mu_1} \Omega_2(y, k) \cdot \frac{df_2(n, y)}{dy} dy \right] + \frac{1}{2} \sqrt{p} H_0 B_0 \left[\int_0^{\mu_1} \Omega_1(y) \cdot \frac{df_2(n, y)}{dy} dy - \Omega_1(\mu_1) \cdot f_2(n, \mu_1) \right] + \frac{2}{p\pi} \left[\Omega_3(\mu_1) \cdot f_2(n, \mu_1) - \int_0^{\mu_1} \Omega_3(y) \cdot \frac{df_2(n, y)}{dy} dy \right] - \frac{2 \sin(n\mu_1\pi)}{pn\pi} \quad (13)$$

with

$$\mu_1 = \xi_1\pi / \beta \quad (14)$$

$$\Omega_1(x) = \int_0^x f_1(u, x) u du \quad (15)$$

$$\Omega_2(x, k) = \int_0^x f_1(u, x) \sin(ku) du \quad (16)$$

$$\Omega_3(x) = \int_0^x f_1(u, x) f_3(u, x) du \quad (17)$$

$$\lambda_n = \sqrt{\left(\frac{n\pi\alpha}{\beta}\right)^2 + p} \quad (18)$$

$$H(n, p) = H_n = K_1(\lambda_n) / K_0(\lambda_n) \quad (19)$$

$$f_1(x, a) = \frac{\sqrt{2} \sin(x/2)}{\pi \sqrt{\cos(x/2) - \cos(a)}} \quad (20)$$

$$f_2(n, a) = [P_n(\cos a) + P_{n-1}(\cos a)] \quad (21)$$

$$f_3(x, a) = \frac{1}{4} (\ln(1 - \cos(a+x)) - \ln(1 - \cos(a-x))) \quad (22)$$

$$I(n, p) = I_n = n - \lambda_n H(n, p) \quad (23)$$

and

$$\lambda_n = \sqrt{\left(\frac{n\pi\alpha}{\beta}\right)^2 + p} \quad (24)$$

where K_0 and K_1 are the modified Bessel functions of the second kind with order zero and one, respectively, and the $P_n(\cos a)$ is the associated Legendre function [Abramowitz and Stegun, 1970, p.335].

The flux entering the well screen and the total well discharge obtained using Eq. (11) are respectively given as:

$$\bar{q}^*(1, \xi, p) = -\frac{\partial \bar{s}^*(1, \xi, p)}{\partial \rho} = \frac{1}{2} B(0, p) \sqrt{p} H_0 + \sum_{n=1}^{\infty} B(n, p) \lambda_n H_n \cos(\eta \xi) \quad (25)$$

and

$$Q(p) = \int_{\xi_1}^{\beta} \bar{q}^*(1, \xi, p) d\xi / \lambda = \frac{1}{2} B(0, p) \sqrt{p} H_0 - \sum_{n=1}^{\infty} \frac{\beta}{n\pi\lambda} B(n, p) \lambda_n H_n \sin(n\mu_1) \quad (26)$$

where $\lambda = l / r_w$ is the dimensionless length of screen.

3.2 Partially penetrating: arbitrary location of the well screen

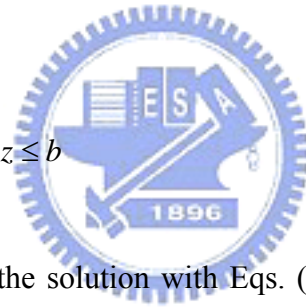
Figure 2 shows a schematic representation of a partially penetrating well in a confined aquifer of finite extent with a finite thickness of b . The well screen which extends from arbitrary location d_1 to d_2 is of length l under a prescribed constant drawdown h_w . In other words, the well screen can be set at any location along the well.

The boundary along the well screen is different from that in section 3.1, which can be written as:

$$s(r_w, z, t) = s_w \quad d_1 \leq z \leq d_2 \quad (27)$$

and

$$\left. \frac{\partial s}{\partial r} \right|_{r=r_w} = 0 \quad 0 \leq z \leq d_1, \quad d_2 \leq z \leq b \quad (28)$$



The detail derivation for the solution with Eqs. (27) and (28) using Laplace transform, finite Fourier cosine transform, and triple series equations method is given in Appendix B.

The solution for drawdown in an aquifer involving a partially penetrating well with arbitrary location of well screen has the same expression as Eq. (11) and the coefficients $B(0, p)$ and

$B(n, p)$ are written as

$$\begin{aligned} B(0, p) &= C(0, p) + D(0, p) \\ &= C_0 + D_0 \end{aligned} \quad (29)$$

and

$$\begin{aligned} B(n, p) &= C(n, p) + D(n, p) \\ &= C_n + D_n \end{aligned} \quad (30)$$

The coefficients in (29) and (30) can be calculated by the following equations

$$C_0 = \left(1 + \sqrt{p}H_0\Omega_1(\mu_1)\right)^{-1} \cdot \left[\frac{4}{p\pi}\Omega_3(\mu_1) + \frac{2}{p}(1 - \mu_1) + \sum_{k=1}^{\infty} \frac{2}{k} I_k (C_k - D_k)\Omega_2(\mu_1, k) - 2D_0\sqrt{p}H_0\Omega_1(\mu_1) \right] \quad (31)$$

$$C_n = \sum_{k=1}^{\infty} \frac{1}{k} (I_k C_k - \lambda_k D_k) \left[\Omega_2(\mu_1, k) \cdot f_2(n, \mu_1) - \int_0^{\mu_1} \Omega_2(y, k) \cdot \frac{df_2(n, y)}{dy} dy \right] + \frac{1}{2}\sqrt{p}H_0(C_0 + D_0) \left[\int_0^{\mu_1} \Omega_1(y) \cdot \frac{df_2(n, y)}{dy} dy - \Omega_1(\mu_1) \cdot f_2(n, \mu_1) \right] + \frac{2}{p\pi} \left[\Omega_3(\mu_1) \cdot f_2(n, \mu_1) - \int_0^{\mu_1} \Omega_3(y) \cdot \frac{df_2(n, y)}{dy} dy \right] - \frac{2\sin(n\mu_1\pi)}{pn\pi} \quad (32)$$

$$D_0 = \left(1 + \sqrt{p}H_0\Omega_1(\mu_2)\right)^{-1} \left[\sum_{k=1}^{\infty} \frac{2}{k} \Omega_2(\mu_2, k) (I_k - (-1)^k \lambda_k H_k) D_k - 2D_0\sqrt{p}H_0\Omega_1(\mu_2, k) \right] \quad (33)$$

and

$$D_n = (-1)^n \sum_{k=1}^{\infty} (-1)^k \frac{1}{k} (I_k D_k - \lambda_k H_k C_k) \cdot \left[\Omega_2(\mu_2, k) \cdot f_2(n, \mu_2) - \int_0^{\mu_2} \Omega_2(y, k) \cdot \frac{df_2(n, y)}{dy} dy \right] + \frac{1}{2}\sqrt{p}H_0(D_0 - C_0) \left[\int_0^{\mu_2} \Omega_1(y) \cdot \frac{df_2(n, y)}{dy} dy - \Omega_1(\mu_2) \cdot f_2(n, \mu_2) \right] \quad (34)$$

$$\mu_2 = \pi(1 - \xi_2 / \beta) \quad (35)$$

The flux entering the well screen and the total well discharge are respectively given as:

$$\bar{q}^*(1, \xi, p) = -\left. \frac{\partial \bar{s}^*(\rho, \xi, p)}{\partial \rho} \right|_{\rho=1} = \frac{1}{2} B_0 \sqrt{p} H_0 + \sum_{n=1}^{\infty} B_n \lambda_n H_n \cos(\eta \xi) \quad (36)$$

and

$$Q(p) = \frac{1}{\lambda} \int_{\xi_1}^{\xi_2} \bar{q}^*(1, \xi, p) d\xi = \frac{1}{2} B_0 \sqrt{p} H_0 - \sum_{n=1}^{\infty} (\lambda \eta)^{-1} B_n \lambda_n H_n [\sin(n\mu_1) + (-1)^n \sin(n\mu_2)] \quad (37)$$

CHAPTER 4 RESULTS AND DISCUSSION

4.1 Simplified solution

When the well fully penetrates the entire thickness of the formation, i.e., ξ_1 is zero and ξ_2 equals β , the drawdown and the well discharge can be obtained using Eqs. (11) and (37), respectively, with coefficients in Eqs. (31) – (34) as

$$\bar{s}^*(\rho, \xi, p) = \frac{1}{p} \psi_0 \quad (38)$$

and

$$Q(p) = \frac{H_0}{\sqrt{p}} \quad (39)$$

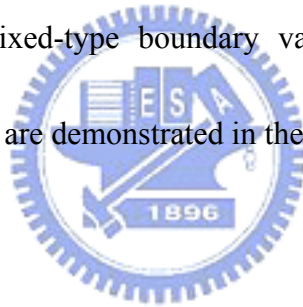
Equations (38) and (39) are identical to the solutions of drawdown and flow rate in Laplace domain given in Yang and Yeh [2006].



4.2 Numerical evaluations

Equation (11) contains single and double infinite series which consist of the summations of multiplication of integrals, trigonometric functions, and the modified Bessel functions of second kind. The integrals are in terms of trigonometric functions multiplying associated Legendre functions. This solution involves numerous complicated mathematical functions. Therefore, numerical approaches including the Gaussian quadrature [Gerald and Wheatley, 1989], Shanks' transform and Stehfest method are proposed to evaluate the solution. The Gaussian quadrature with 6 terms [Yang and Yeh, 2007] is first utilized to evaluate the

integrals in Eq. (11). Since the oscillation and slow convergence of the multiplication terms, the summations are difficult to evaluate accurately and efficiently. Therefore, the Shanks' transform method [Shanks, 1955], a nonlinear iterative algorithm based on the sequence of partial sums, is used to compute the summations in Eq. (11). This method has been successfully devoted to efficiently computing the solutions arisen in the groundwater area [see, e.g., Peng et al. 2002; Yeh et al. 2003]. In addition, the Stehfest algorithm [Stehfest, 1970] with eight weighting factors is further employed to inverse the Laplace domain solution into time domain solution. The proposed numerical approaches can accurately evaluate the drawdown solution to the mixed-type boundary value problem for a flowing partially penetrating well and the results are demonstrated in the following section.



4.3 Drawdown and well bore flux distribution

Figure 3 shows the dimensionless drawdown for $\beta = 100$, $\xi_1 = 50$, $\xi_2 = 100$ and various ρ at $\tau = 1, 100, 10^4$ and 10^6 . As indicated in the figure, the dimensionless drawdown is constant along the well screen and decreases with increasing dimensionless radial distance at $\tau = 1$. In addition, the dimensionless drawdown increases with dimensionless time along the unscreened part of the well. Figure 4 shows the plots of the flux along the well screen for $\beta = 100$, $\xi_1 = 50$ and $\xi_2 = 100$ at $\tau = 1, 100, 10^4$ and 10^6 . The dimensionless flux is non-uniformly distributed and large at the screen edge. The

vertical flow is induced by the presence of well partial penetration and the maximum flux at the screen edge occurs when the vertical flows enter the bottom of the well. The spatial dimensionless drawdown contours at $\tau = 100$, 10^3 and 10^4 are plotted in Figure 5. The dimensionless drawdown increases with dimensionless time at a fixed radial distance and flow is horizontal when the dimensionless radial distance is large than 80 and the dimensionless time is 10^4 . Figures 6(a) and 6(b) show the spatial dimensionless drawdown contours for various α^2 with $\xi_1 = 200$ and $\xi_2 = 250$ at $\tau = 10^5$ and demonstrates the influence of anisotropy on the dimensionless drawdown. The flow is almost horizontal at lower part of the aquifer when the dimensionless radial distance is large than 400 for $\alpha^2 = 1$ and the vertical flow appears at lower part of the aquifer for $\alpha^2 = 0.5$. Figures 7(a) and 7(b) show the spatial dimensionless drawdown contours with same length of 50 but different locations of well screen. In Figure 7(a), the screen is symmetric with $\xi_1 = 12.5$ and $\xi_2 = 37.5$ and in Figure 7(b) the screen extends from the top of the aquifer with $\xi_1 = 25$ and $\xi_2 = 50$ at $\tau = 10^5$. Since the screen is symmetric about the middle line of the aquifer, the drawdown contours are symmetric as demonstrated in Figure 7(a). Figure 8 illustrates the spatial dimensionless drawdown contours for $\xi_1 = 100$ and $\xi_2 = 150$ at $\tau = 10^7$ in an infinite aquifer. On the upper part of the aquifer, the direction of flow is downward when the radial distance is far from the test well and it is upward when the radial distance is close to the well screen. Since the aquifer is infinite, the drawdown at the upper screen ledge flows



upward and then flows toward the bottom of the aquifer and the drawdown at the lower screen ledge flows down toward the bottom of the aquifer.

4.4 Effect of penetration ratio

In order to explore the effect of partial penetration on the well discharge, Figure 9 illustrates the behavior of well discharge in response to four different penetration ratios $\omega = \lambda / \beta$ with $\lambda = 50$. The well discharges responding to those four cases behave the same at the small time; however, it decreases with increasing penetration ratio at large time.

If the penetration ratio is smaller than 0.01, the well discharge of this study agrees with that of constant head pumping test in Cassiani et al.[1999] in an aquifer of semi-infinite thickness.

In other words, if the aquifer thickness is greater than 100 times of the screen length, the aquifer can be considered as a semi-infinite aquifer. As the penetration ratio is equal to 1,

the well discharge of this study is identical to that of Yang and Yeh [2006] for a fully

penetrating well. In addition, well discharges of this study agree with those of Chang and

Chen [2003] for $\omega = 0.01$ and $\omega = 0.001$ when $\lambda = 50$. As indicated in Figure 9, there

are no obvious differences in the well discharges in response to different penetration ratios

until $\tau = 10^4$. For the cases of $\omega = 0.1$ and $\omega = 0.01$, the flow caused by the partial

penetration did not reach to the bottom of the aquifer before $\tau = 10^4$. The aquifer thickness

has influence on groundwater flow after τ is greater than 10^4 . The well discharge for

$\omega = 0.01$ is stabilized as τ increases to 10^6 and the well discharge for $\omega = 0.5$ continues to decrease.



CHAPTER 5 CONCLUSIONS

This paper developed new semi-analytical solutions for the aquifer system in response to the constant head test at a partially penetrating well in a confined aquifer of infinite radial extent and finite vertical extent. The Laplace and finite cosine Fourier transforms is first used to reduce the original partial differential equation with mixed-type boundary and initial conditions for a partially penetrating well in an aquifer of finite thickness to the dual or triple series equations.

The present solutions for a fully penetrating well in an aquifer of finite thickness are identical to the solutions of the drawdown and well discharge given in Chen and Stone [1993]. It is found that the solution of Cassiani et al. [1999] for well response to a constant head pumping test in a semi-infinite aquifer approximates the solution for the case where the aquifer thickness of a finite aquifer is 100 times greater than the length of well screen. In addition, the flux is non-uniformly distributed along the screen and with a local peak at the edge, due to the vertical flow induced by well partial penetration.

The new semi-analytical solutions provide accurate description of the response of the aquifer system to a constant head pumping test performed at a partially penetrating well in a confined aquifer of infinite radial extent and finite vertical extent. Those solutions are particularly attractive for practical applications since they can be used to evaluate the

sensitivities of the input parameters in a mathematical model. In addition, the solution can be used to calculate the flow rates during the constant-head test and plots specific drawdown (drawdown divided by the flow rate) versus time to identify the hydraulic parameters if coupling with an optimization approach in the analysis of aquifer data, and to verify a numerical solution.



APPENDIX A

The Laplace and finite cosine Fourier transforms are first used to solve the mixed-type boundary value problem. The definition of Laplace transform is [Sneddon, 1972] :

$$\bar{s}^*(\rho, \xi, p) = L_p[s^*(\rho, \xi, \tau); \tau \rightarrow p] = \int_0^{\infty} s^*(\rho, \xi, \tau) e^{-p\tau} d\tau \quad (\text{A1})$$

where $\bar{s}^*(\rho, \xi, p)$ is the dimensionless drawdown in Laplace domain. Taking the Laplace transform of Eqs. (6) and (8) – (10) and using the initial condition in Eq. (7), the problem reads:

$$\frac{\partial^2 \bar{s}^*}{\partial \rho^2} + \frac{1}{\rho} \frac{\partial \bar{s}^*}{\partial \rho} + \alpha^2 \frac{\partial^2 \bar{s}^*}{\partial \xi^2} - p \bar{s}^* = 0 \quad (\text{A2})$$

$$\bar{s}^*(\rho = \infty, \xi, p) = 0 \quad (\text{A3})$$

$$\bar{s}^*(\rho = 1, \xi, p) = \frac{1}{p}, \quad \xi_1 \leq \xi \leq \beta \quad (\text{A4a})$$

$$\left. \frac{\partial \bar{s}^*}{\partial \rho} \right|_{\rho=1} = 0, \quad 0 \leq \xi \leq \xi_1 \quad (\text{A4b})$$

$$\frac{\partial \bar{s}^*}{\partial \xi} = 0, \quad \xi = 0, \xi = \beta \quad (\text{A5})$$

In order to eliminate the ξ coordinate, the finite cosine Fourier transform is used as follows [Sneddon, 1972]:

$$\hat{s}^*(\rho, n, p) = F_c[\bar{s}^*(\rho, \xi, p); \xi \rightarrow n] = \int_0^{\beta} \bar{s}^*(\rho, \xi, p) \cos(n\xi) d\xi \quad (\text{A6})$$

where $\hat{s}^*(\rho, n, p)$ is the dimensionless drawdown after finite cosine Fourier transform.

Substituting Eq. (A6) into Eqs. (A2), (A3) and (A5) results in the Bessel differential equation

as

$$\frac{\partial^2 \hat{s}^*}{\partial \rho^2} + \frac{1}{\rho} \frac{\partial \hat{s}^*}{\partial \rho} - \lambda_n^2 \hat{s}^* = 0 \quad (\text{A7})$$

with the boundary condition

$$\hat{s}^*(\rho = \infty, n, p) = 0 \quad (\text{A8})$$

where λ_n is defined in Eq. (24).

The general solution of Eq. (A7) with the boundary condition Eq. (A8) is [Carslaw and Jaeger, 1959, p. 193]

$$\hat{s}^*(\rho, n, p) = A(n, p)K_0(\lambda_n \rho) \quad (\text{A9})$$

where $A(n, p)$ can be found from using the mixed-type boundary condition Eq. (A4). The inverse of the finite cosine Fourier transform is [Sneddon, 1972, p.425]

$$\bar{s}^*(\rho, \xi, p) = \frac{1}{\beta} \hat{s}^*(\rho, 0, p) + \frac{2}{\beta} \sum_{n=1}^{\infty} \hat{s}^*(\rho, n, p) \cos(\eta \xi) \quad (\text{A10})$$

Thus, the solution in ξ domain obtained by inserting Eq. (A9) into Eq. (A10) is

$$\bar{s}^*(\rho, \xi, p) = \frac{1}{\beta} A(0, p)K_0(\sqrt{p}\rho) + \frac{2}{\beta} \sum_{n=1}^{\infty} A(n, p)K_0(\lambda_n \rho) \cos(\eta \xi) \quad (\text{A11})$$

with its derivative with respect to ρ given by

$$\frac{\partial \bar{s}^*}{\partial \rho}(\rho, \xi, p) = -\frac{1}{\beta} A(0, p)\sqrt{p}K_1(\sqrt{p}\rho) - \frac{2}{\beta} \sum_{n=1}^{\infty} A(n, p)\lambda_n K_1(\lambda_n \rho) \cos(\eta \xi) \quad (\text{A12})$$

Substituting Eq. (A11) into Eq. (A4a) and Eq. (A12) into Eq. (A4b) results in a system of the

dual series equations (DSE)

$$\frac{1}{\beta} A(0, p)K_0(\sqrt{p}) + \frac{2}{\beta} \sum_{n=1}^{\infty} A(n, p)K_0(\lambda_n) \cos(\eta \xi) = \frac{1}{p}, \xi_1 \leq \xi \leq \beta \quad (\text{A13a})$$

$$\frac{1}{\beta} A(0, p)\sqrt{p}K_1(\sqrt{p}) + \frac{2}{\beta} \sum_{n=1}^{\infty} A(n, p)\lambda_n K_1(\lambda_n) \cos(\eta \xi) = 0, 0 \leq \xi \leq \xi_1 \quad (\text{A13b})$$

We define that

$$B(n, p) = 2A(n, p)K_0(\lambda_n) / \beta \quad (\text{A14})$$

The DSE of (A13) can be arranged as [Sneddon, 1966, p.161]:

$$\frac{1}{2}B(0, p) + \sum_{n=1}^{\infty} B(n, p) \cos(nx) = \frac{1}{p}, \quad \mu_1 < x \leq \pi \quad (\text{A15a})$$

$$\frac{1}{2}B(0, p)\sqrt{p}H(0, p) + \sum_{n=1}^{\infty} nB(n, p) \cos(nx) = \sum_{k=1}^{\infty} I(k, p)B(k, p) \cos(kx), \quad 0 \leq x \leq \mu_1 \quad (\text{A15b})$$

with $x = \xi\pi / \beta$.

Our goal is to determine the coefficients $B(0, p)$ and $B(n, p)$ appearing in Eq. (A15). The pair of dual series equations (DSE) can be solved by following the procedure given in Sneddon

[1966]. Assume that when $0 \leq x \leq \mu_1$

$$\frac{1}{2}B_0 + \sum_{n=1}^{\infty} B_n \cos(nx) = \cos\left(\frac{x}{2}\right) \int_x^{\mu_1} \frac{h_1(y)dy}{\sqrt{\cos x - \cos y}} \quad (\text{A16})$$

where $\mu_1 = \xi_1\pi / \beta$, $B_0 = B(0, p)$ and $B_n = B(n, p)$.

The coefficient B_0 and B_n in Eq. (A15) are respectively given by the equations [Sneddon, 1966, p. 161, Eqs. (5.4.56) and (5.4.57)]

$$B_0 = \frac{2}{\pi} \left[\frac{\pi}{\sqrt{2}} \int_0^{\mu_1} h_1(y)dy \right] \quad (\text{A17})$$

and

$$B_n = \frac{2}{\pi} \left\{ \frac{\pi}{2\sqrt{2}} \int_0^{\mu_1} h_1(y) [P_n(\cos y) + P_{n-1}(\cos y)] dy \right\} \quad (\text{A18})$$

Integrating (A15b), one can obtain

$$\begin{aligned} & \frac{1}{2}B_0\sqrt{p}H(0, p)x + \sum_{n=1}^{\infty} B_n \sin(nx) \\ &= \int_0^x \left(\sum_{n=1}^{\infty} B_n I_n \cos(nu) \right) du = \int_0^x F(u) du \end{aligned} \quad (\text{A19})$$

Substituting Eqs. (A17) and (A18) into (A19), one can find that $h_1(y)$ satisfies the following

equation: [Sneddon, 1966, p. 161, Eq. (5.4.58)]

$$\int_0^{\mu_1} h_1(y) \frac{1}{\sqrt{2}} \sum_{n=1}^{\infty} [P_n(\cos y) + P_{n-1}(\cos y)] \sin nx dy = \int_0^x F(u) du - \frac{1}{2} \sqrt{p} H(0, p) B_0 x - \sum_{n=1}^{\infty} \frac{2}{\pi} \int_{\mu_1}^{\pi} \frac{1}{p} \cos(nu) du \sin(nx) \quad (\text{A20})$$

The summation term on the left-hand side of Eq. (A20) can be expressed as [Sneddon, 1966, p. 59, Eq. (2.6.31)]

$$\frac{1}{\sqrt{2}} \sum_{n=1}^{\infty} [P_n(\cos y) + P_{n-1}(\cos y)] \sin nx = \frac{\cos\left(\frac{x}{2}\right) H_{eav}(x-y)}{\sqrt{\cos y - \cos x}} \quad (\text{A21})$$

where $H_{eav}(X)$ is the Heaviside unit step function which is of different value for different

range of X such as

$$H_{eav}(X) = \begin{cases} 0 & X < 0 \\ 1/2 & X = 0 \\ 1 & X > 0 \end{cases} \quad (\text{A22})$$



Substituting (A21) into (A20), it yields

$$\int_0^{\mu_1} \frac{h_1(y) H(x-y)}{\sqrt{\cos y - \cos x}} dy = \sec \frac{x}{2} \left\{ \int_0^x F(u) du - \frac{1}{2} \sqrt{p} H(0, p) B_0 x - \sum_{n=1}^{\infty} \frac{2}{\pi} \int_{\mu_1}^{\pi} \frac{1}{p} \cos(nu) du \sin(nx) \right\} \quad (\text{A23})$$

Using the property of Heaviside unit step function in Eq. (A22), an equivalent integral

equation of (A23) can be obtained

$$\int_0^x \frac{h_1(y)}{\sqrt{\cos y - \cos x}} dy = \sec \frac{x}{2} \left\{ \int_0^x F(u) du - \frac{1}{2} \sqrt{p} H(0, p) B_0 x - \sum_{n=1}^{\infty} \frac{2}{\pi} \int_{\mu_1}^{\pi} \frac{1}{p} \cos(nu) du \sin(nx) \right\} \quad (\text{A24})$$

Then, the function $h_1(y)$ can be found based on Sneddon [1966, p. 41, Eq. (2.3.5)] as

$$h_1(y) = \frac{2}{\pi} \frac{d}{dy} \int_0^y \frac{\sin(x/2)}{\sqrt{\cos x - \cos y}} \left\{ \int_0^x F(u) du - \frac{1}{2} \sqrt{p} H(0, p) B_0 x - \sum_{n=1}^{\infty} \frac{2}{\pi} \int_{\mu_1}^{\pi} \frac{1}{p} \cos(nu) du \sin(nx) \right\} dx \quad (\text{A25})$$

By integrating Eq. (A25) and substituting it into Eqs. (A17) and (A18), the coefficients B_0 and B_n can be expressed as Eqs. (12) and (13), respectively.

For computational convenience, the coefficients can be written in the matrix form as

$$\begin{bmatrix} B_0 \\ B_1 \\ B_2 \\ \vdots \\ B_n \end{bmatrix} = \begin{bmatrix} 0 & X_{12} & X_{13} & \cdots & X_{1,n+1} \\ 0 & X_{22} & X_{23} & \cdots & X_{2,n+1} \\ 0 & X_{32} & X_{33} & \cdots & X_{3,n+1} \\ \vdots & \vdots & \vdots & \ddots & \vdots \\ 0 & X_{n+1,2} & X_{n+1,3} & \cdots & X_{n+1,n+1} \end{bmatrix} \begin{bmatrix} B_0 \\ B_1 \\ B_2 \\ \vdots \\ B_n \end{bmatrix} + \begin{bmatrix} Z_1 \\ Z_2 \\ Z_3 \\ \vdots \\ Z_{n+1} \end{bmatrix} \quad (\text{A26})$$



with

$$X_{i1} = \frac{1}{2} \sqrt{p} H_0 \left[\int_0^{\mu_1} \Omega_1(y) \cdot \frac{df_2(i-1, y)}{dy} dy - \Omega_1(\mu_1) \cdot f_2(i-1, \mu_1) \right] \quad (\text{A27})$$

$$X_{ij} = \frac{1}{(j-1)} I_{j-1} \left[\Omega_2(\mu_1, i-1) \cdot f_2(i-1, \mu_1) - \int_0^{\mu_1} \Omega_2(y, i-1) \cdot \frac{df_2(i-1, y)}{dy} dy \right] + \frac{1}{2} \sqrt{p} H_0 \left[\int_0^{\mu_1} \Omega_1(y) \cdot \frac{df_2(i-1, y)}{dy} dy - \Omega_1(\mu_1) \cdot f_2(i-1, \mu_1) \right] \quad (\text{A28})$$

$$Z_1 = \frac{\frac{4}{p\pi} \Omega_3(\mu_1) + \frac{2}{p} (1 - \mu_1)}{1 + \sqrt{p} H_0 \Omega_1(\mu_1)} \quad (\text{A29})$$

$$Z_i = \frac{2}{p\pi} \left[\Omega_3(\mu_1) \cdot f_2(i-1, \mu_1) - \int_0^{\mu_1} \Omega_3(y) \cdot \frac{df_2(i-1, y)}{dy} dy \right] - \frac{2 \sin((i-1)\mu_1)}{(i-1)\pi p} \quad (\text{A30})$$

where i and j goes from 1 to n .

APPENDIX B

Similar to the procedure in Appendix A, the problem with the boundary in Eqs. (27) and

(28) results in a set of triple series equations as

$$\frac{1}{2}B(0, p) + \sum_{n=1}^{\infty} B(n, p) \cos(nx) = \frac{1}{p}, \quad \mu_1 < x \leq \pi - \mu_2 \quad (\text{B1a})$$

$$\frac{1}{2}B(0, p)\sqrt{p}H(0, p) + \sum_{n=1}^{\infty} B(n, p)\lambda_n H_n \cos(nx) = 0, \quad 0 \leq x \leq \mu_1, \quad \pi - \mu_2 \leq x \leq \pi \quad (\text{B1b})$$

We split Eq. (B1) into the following equations

$$\frac{1}{2}(C_0 + D_0)\sqrt{p}H(0, p) + \sum_{n=1}^{\infty} (C_n + D_n)\lambda_n H_n \cos(nx) = 0, \quad 0 \leq x \leq \mu_1 \quad (\text{B2a})$$

$$\frac{1}{2}C_0 + \sum_{n=1}^{\infty} C_n \cos(nx) = \frac{1}{p}, \quad \mu_1 < x \leq \pi \quad (\text{B2b})$$

$$\frac{1}{2}D_0 + \sum_{n=1}^{\infty} D_n \cos(nx) = 0, \quad 0 < x \leq \pi - \mu_2 \quad (\text{B3a})$$

$$\frac{1}{2}(C_0 + D_0)\sqrt{p}H(0, p) + \sum_{n=1}^{\infty} (C_n + D_n)\lambda_n H_n \cos(nx) = 0, \quad \pi - \mu_2 \leq x \leq \pi \quad (\text{B3b})$$

Equations (B2) and (B3) can be regarded as dual series relations by means of which the coefficients C_0, D_0, C_n and D_n can be determined.

The pair of dual series equations (DSE), i.e., Eq. (B2), can be solved by the procedure given in Appendix A and the coefficients can be written in the matrix form as

$$\begin{aligned}
\begin{bmatrix} C_0 \\ C_1 \\ C_2 \\ \vdots \\ C_n \end{bmatrix} &= \begin{bmatrix} 0 & X_{12} & X_{13} & \cdots & X_{1,n+1} \\ 0 & X_{22} & X_{23} & \cdots & X_{2,n+1} \\ 0 & X_{32} & X_{33} & \cdots & X_{3,n+1} \\ \vdots & \vdots & \vdots & \ddots & \vdots \\ 0 & X_{n+1,2} & X_{n+1,3} & \cdots & X_{n+1,n+1} \end{bmatrix} \begin{bmatrix} C_0 \\ C_1 \\ C_2 \\ \vdots \\ C_n \end{bmatrix} \\
&+ \begin{bmatrix} Y_{11} & Y_{12} & Y_{13} & \cdots & Y_{1,n+1} \\ Y_{21} & Y_{22} & Y_{23} & \cdots & Y_{2,n+1} \\ Y_{31} & Y_{32} & Y_{33} & \cdots & Y_{3,n+1} \\ \vdots & \vdots & \vdots & \ddots & \vdots \\ Y_{n+1,1} & Y_{n+1,2} & Y_{n+1,3} & \cdots & Y_{n+1,n+1} \end{bmatrix} \begin{bmatrix} D_0 \\ D_1 \\ D_2 \\ \vdots \\ D_n \end{bmatrix} \\
&+ \begin{bmatrix} Z_1 \\ Z_2 \\ Z_3 \\ \vdots \\ Z_{n+1} \end{bmatrix}
\end{aligned} \tag{B4}$$

with

$$X_{i1} = \frac{1}{2} \sqrt{p} H_0 \left[\int_0^{\mu_1} \Omega_1(y) \cdot \frac{df_2(i-1, y)}{dy} dy - \Omega_1(\mu_1) \cdot f_2(i-1, \mu_1) \right] \tag{B5}$$

$$\begin{aligned}
X_{ij} &= \frac{1}{(j-1)} I_{j-1} \left[\Omega_2(\mu_1, i-1) \cdot f_2(i-1, \mu_1) - \int_0^{\mu_1} \Omega_2(y, i-1) \cdot \frac{df_2(i-1, y)}{dy} dy \right] \\
&+ \frac{1}{2} \sqrt{p} H_0 \left[\int_0^{\mu_1} \Omega_1(y) \cdot \frac{df_2(i-1, y)}{dy} dy - \Omega_1(\mu_1) \cdot f_2(i-1, \mu_1) \right]
\end{aligned} \tag{B6}$$

$$Y_{11} = \frac{-\sqrt{p} H_0 \Omega_1(\mu_1)}{1 + \sqrt{p} H_0 \Omega_1(\mu_1)} \tag{B7}$$

$$Y_{1j} = \frac{\frac{-2}{(j-1)} \lambda_{j-1} H_{j-1} \Omega_2(\mu_1, j-1)}{1 + \sqrt{p} H_0 \Omega_1(\mu_1)} \tag{B8}$$

$$Y_{i1} = \frac{1}{2} \sqrt{p} H_0 \left[\int_0^{\mu_1} \Omega_1(y) \cdot \frac{df_2(i-1, y)}{dy} dy - \Omega_1(\mu_1) \cdot f_2(i-1, \mu_1) \right] \tag{B9}$$

$$Y_{ij} = \frac{1}{(j-1)} \lambda_{j-1} H_{j-1} \left[\int_0^{\mu_1} \Omega_2(y, j-1) \cdot \frac{df_2(i-1, y)}{dy} dy - \Omega_2(\mu_1, j-1) \cdot f_2(i-1, \mu_1) \right] \tag{B10}$$

$$Z_1 = \frac{\frac{4}{p\pi} \Omega_3(\mu_1) + \frac{2}{p} (1 - \mu_1)}{1 + \sqrt{p} H_0 \Omega_1(\mu_1)} \tag{B11}$$

$$Z_i = \frac{2}{p\pi} \left[\Omega_3(\mu_1) \cdot f_2(i-1, \mu_1) - \int_0^{\mu_1} \Omega_3(y) \cdot \frac{df_2(i-1, y)}{dy} dy \right] - \frac{2 \sin((i-1)\mu_1)}{(i-1)\pi p} \quad (\text{B12})$$

where i and j goes from 1 to n .

Similarly, Eq. (B3) can be solved by setting $x' = \pi - x$ and $D_n' = (-1)^n D_n$. Equation

(B3) is rewritten as

$$\frac{1}{2} D_0' + \sum_{n=1}^{\infty} D_n' \cos(nx') = 0, \quad \mu_2 < x' \leq \pi \quad (\text{B13a})$$

$$\frac{1}{2} (D_0' + C_0) \sqrt{p} H_0 + \sum_{n=1}^{\infty} (D_n' + (-1)^n C_n) \lambda_n H_n \cos(nx') = 0, \quad 0 \leq x' \leq \mu_2 \quad (\text{B13b})$$

and the coefficients D_0 and D_n are

$$\begin{bmatrix} D_0 \\ D_1 \\ D_2 \\ \vdots \\ D_n \end{bmatrix} = \begin{bmatrix} 0 & XX_{12} & XX_{13} & \cdots & XX_{1,n+1} \\ 0 & XX_{22} & XX_{23} & \cdots & XX_{2,n+1} \\ 0 & XX_{32} & XX_{33} & \cdots & XX_{3,n+1} \\ \vdots & \vdots & \vdots & \ddots & \vdots \\ 0 & XX_{n+1,2} & XX_{n+1,3} & \cdots & XX_{n+1,n+1} \end{bmatrix} \begin{bmatrix} D_0 \\ D_1 \\ D_2 \\ \vdots \\ D_n \end{bmatrix} + \begin{bmatrix} YY_{11} & YY_{12} & YY_{13} & \cdots & YY_{1,n+1} \\ YY_{21} & YY_{22} & YY_{23} & \cdots & YY_{2,n+1} \\ YY_{31} & YY_{32} & YY_{33} & \cdots & YY_{3,n+1} \\ \vdots & \vdots & \vdots & \ddots & \vdots \\ YY_{n+1,1} & YY_{n+1,2} & YY_{n+1,3} & \cdots & YY_{n+1,n+1} \end{bmatrix} \begin{bmatrix} C_0 \\ C_1 \\ C_2 \\ \vdots \\ C_n \end{bmatrix} \quad (\text{B14})$$

with the elements

$$XX_{1j} = \frac{2(-1)^{j-1}}{(j-1)} \frac{I_{j-1} \Omega_2(\mu_2, j-1)}{1 + \sqrt{p} H_0 \Omega_1(\mu_2)} \quad (\text{B15})$$

$$XX_{ij} = \frac{\sqrt{2}}{\pi} \frac{(-1)^{i-1} (-1)^{j-1}}{(j-1)} I_{j-1} \left[\Omega_2(\mu_2, j-1) \cdot f_2(i-1, \mu_2) - \int_0^{\mu_2} \Omega_2(y, j-1) \cdot \frac{df_2(i-1, y)}{dy} dy \right] \quad (\text{B16})$$

$$YY_{11} = \frac{-\sqrt{p} H_0 \Omega_1(\mu_2)}{1 + \sqrt{p} H_0 \Omega_1(\mu_2)} \quad (\text{B17})$$

$$YY_{1j} = \frac{-2}{(j-1)} \frac{\lambda_{j-1} H_{j-1} \Omega_2(\mu_2, j-1)}{1 + \sqrt{p} H_0 \Omega_1(\mu_2)} \quad (\text{B18})$$

$$YY_{i1} = \frac{(-1)^{i-1}}{2} \sqrt{p} H_0 \left[\int_0^{\mu_2} \Omega_1(y) \cdot \frac{df_2(i-1, y)}{dy} dy - \Omega_1(\mu_2) \cdot f_2(i-1, \mu_2) \right] \quad (\text{B19})$$

$$YY_{ij} = \frac{(-1)^{j-1} (-1)^{i-1}}{(j-1)} \lambda_{j-1} H_{j-1} \left[\int_0^{\mu_2} \Omega_2(y, j-1) \cdot \frac{df_2(i-1, y)}{dy} dy - \Omega_2(\mu_2, j-1) \cdot f_2(i-1, \mu_2) \right] \quad (\text{B20})$$



REFERENCES

- Abramowitz, M., and I. A. Stegun (1970), *Handbook of Mathematical Functions*, Dover Publications, New York.
- Bassani, J. L., M.W. Nansteel, and M. November (1987), Adiabatic-isothermal mixed boundary conditions in heat transfer, *J Heat Mass Transfer.*, 30, 903-909.
- Boridy, E., 1990. A perturbation approach to mixed boundary-value spherical problems, *J. Appl. Phys.*, 67, 6682-6666.
- Carslaw, H. S., and J. C. Jaeger (1959), *Conduction of heat in solids*, 2nd Ed., Clarendon, Oxford.
- Cassiani, G., and Z. J. Kabala (1998), Hydraulics of a partially penetrating well: solution to a mixed-type boundary value problem via dual integral equations, *J. Hydrol.*, 211, 100-111.
- Cassiani, G., Z. J. Kabala, and M.A. Medina Jr (1999), Flowing partially penetrating well: solution to a mixed-type boundary value problem, *Adv. Water Resour*, 23, 59-68.
- Chang, C. C., and C.S. Chen (2002), An integral transform approach for a mixed boundary problem involving a flowing partially penetrating well with infinitesimal well skin, *Water Resour. Res.*, 38(6), 1071.
- Chang, C. C., and C.S. Chen (2003), A flowing partially penetrating well in a finite-thickness aquifer: a mixed-type initial boundary value problem, *J. Hydrol.*, 271, 101-118.
- Chang, Y. C. and H. D. Yeh (2009) New solutions to the constant-head test performed at a partially penetrating well, *J. Hydrol.*, doi:10.1016/j.jhydrol.2009.02.016
- Gerald, C. F. and P. O. Wheatley (1989), *Applied numerical analysis*, 4th ed., Addison-Wesley, California.
- Hantush, M. S. (1964), *Hydraulics of wells. Advances in Hydroscience*, 1, edited by V.T. Chow, Academic, San Diego, Calif., 309-343.

- Hung, S. C. and Y. P. Chang (1984), Anisotropic heat conduction with mixed boundary conditions, *J. Heat Transfer*, 106, 646-648.
- Hung, S. C. (1985), Unsteady-state heat conduction in semi-infinite regions with mixed-type boundary conditions, *J. Heat Transfer*, 107, 489-491.
- Jones, L., T. Lemar, and C.T. Tsai (1992), Results of two pumping tests in Wisconsin age weathered till in Iowa, *Ground Water*, 30(4), 529-538.
- Jones, L., T. (1993), A comparison of pumping and slug tests for estimating the hydraulic conductivity of unweathered Wisconsin age till in Iowa, *Ground Water*, 31(6), 896-904.
- Mishra, S. and D. Guyonnet (1992), Analysis of observation-well response during constant-head testing, *Ground Water*, 32(6), 949-957.
- Murdoch, L.D., and J. Franco (1992), The analysis of constant drawdown wells using instantaneous source functions, *Water Resour. Res.*, 30(1), 117-127.
- Noble, B. (1958), *Methods based on the Wiener-Hopf techniques*, Pergamon Press, New York.
- Peng, H. Y., H. D. Yeh, and S. Y. Yang (2002), Improved numerical evaluation for the radial groundwater flow equation, *Adv. Water Resour.*, 25(6), 663-675.
- Rice, J.B (1998) Constant drawdown aquifer tests: an alternative to traditional constant rate tests, *Ground Water Monit. R.*, 18(2), 76-78.
- Shanks D. (1955), Non-linear transformations of divergent and slowly convergent sequence, *J. Math. Phys.*, 34, 1-42.
- Slim, M. S., and D. Kirkham (1974), Screen theory for wells and soil drainpipes, *Water Resour. Res.*, 10(5), 1019-1030.
- Sneddon, I.N. (1966), *Mixed boundary value problems in potential theory*, North-Holland, Amsterdam.
- Sneddon, I.N. (1972), *The use of integral transforms*, McGraw-Hill, New York, 540pp.
- Stehfest, H. (1970), Numerical inversion of Laplace transforms, *Comm. ACM*, 13, 47-49.

- Wilkinson, D., and P. S. Hammond (1990), A perturbation method for mixed boundary-value problems in pressure transient testing, *Trans Porous Media*, 5(6), 609-636.
- Yang, S. Y., and H. D. Yeh (2002), Solution for flow rates across the wellbore in a two-zone confined aquifer, *J. Hydraul. Eng. ASCE*, 128(2), 175-183.
- Yang, S. Y., and H. D. Yeh (2005). Laplace-domain solutions for radial two-zone flow equations under the conditions of constant-head and partially penetrating well, *J. Hydraul. Eng. ASCE*, 131(3), 209-216.
- Yang, S.Y., and H. D. Yeh (2006), A novel analytical solution for constant-head test in a patchy aquifer, *Int. J. Numer. Anal. Methods Geomech*, 30(12), 1213-1230, doi:10.1002/nag.523.
- Yedder, R. B., and E. Bilgen (1994), On adiabatic-isothermal mixed boundary conditions in heat transfer, *Warme Stoffubertragung*, 29, 457-460.
- Yeh, H. D., S. Y. Yang, and H. Y. Peng (2003), A new closed-form solution for a radial two-layer drawdown equation for groundwater under constant-flux pumping in a finite-radius well, *Adv. Water Res.*, 26(7), 747-757.
- Yeh, H. D., and S. Y. Yang (2006), A novel analytical solution for a slug test conducted in a well with a finite-thickness skin, *Adv. Water Resour.*, 29(10), 1479-1489, doi:10.1016/j.advwatres.2005.11.002.

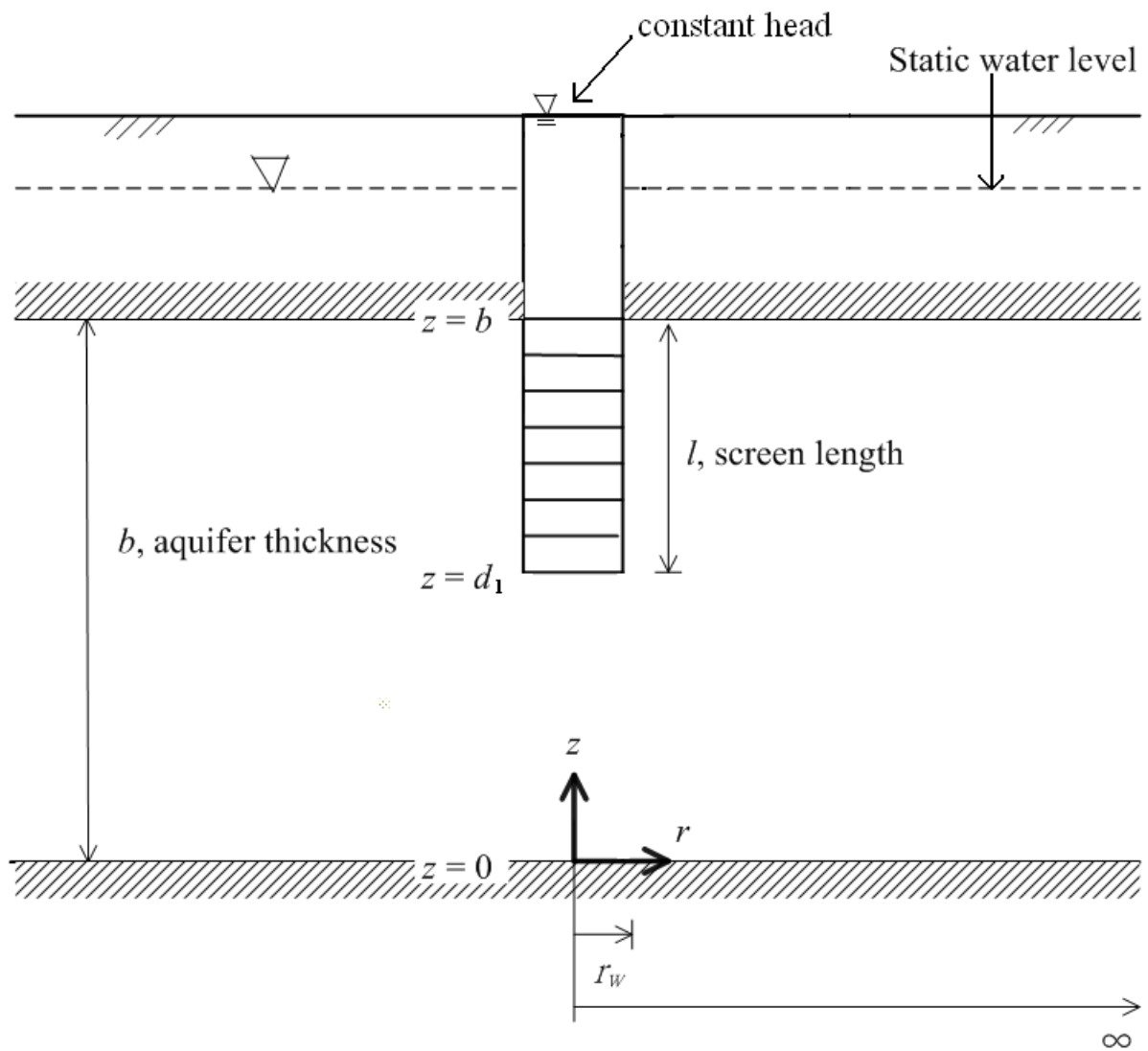


Figure 1 Schematic representation of a partially penetrating well with the screen extends from the top of the aquifer in a confined aquifer

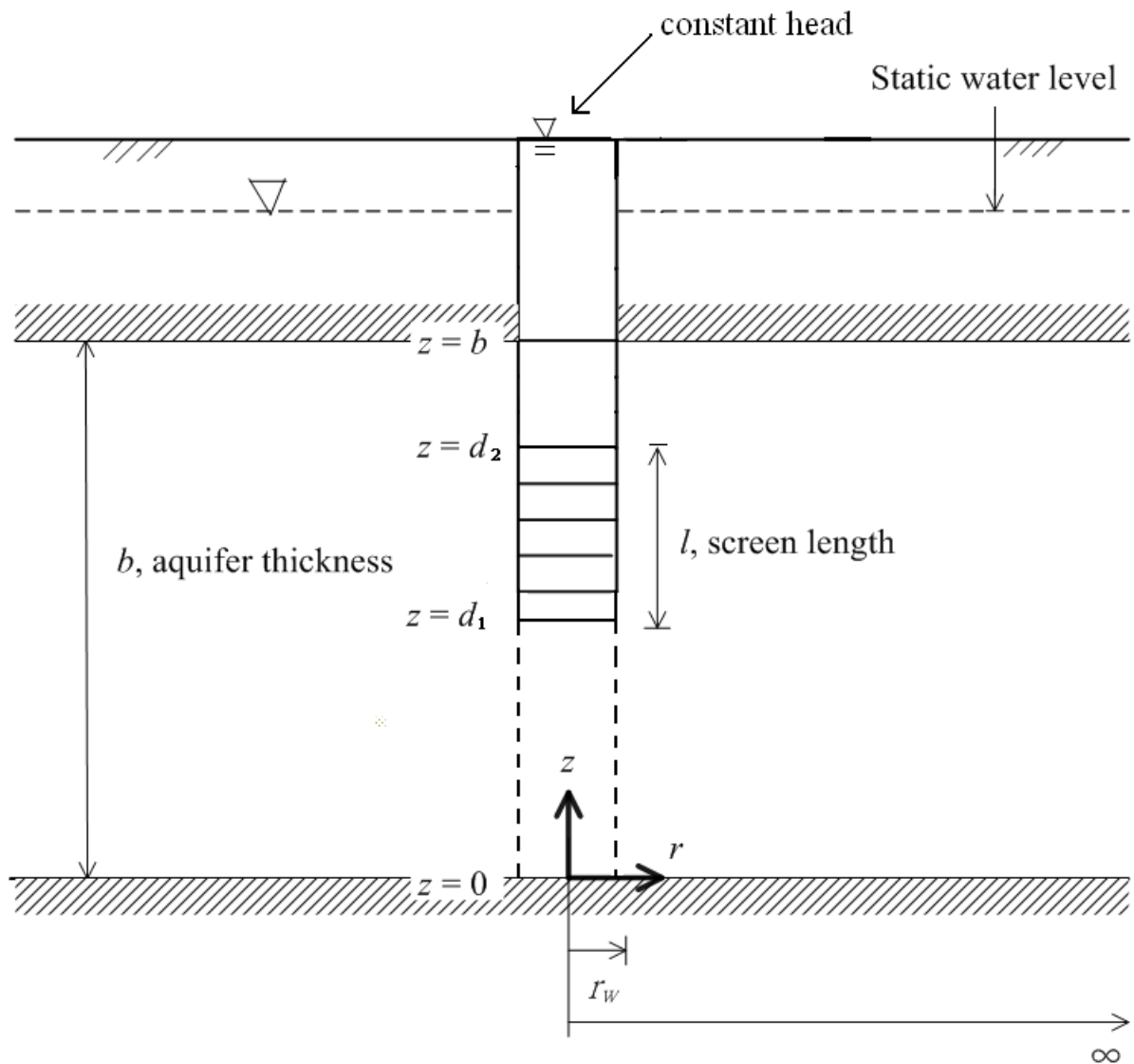


Figure 2 Schematic representation of a partially penetrating well with arbitrary location of well screen in a confined aquifer

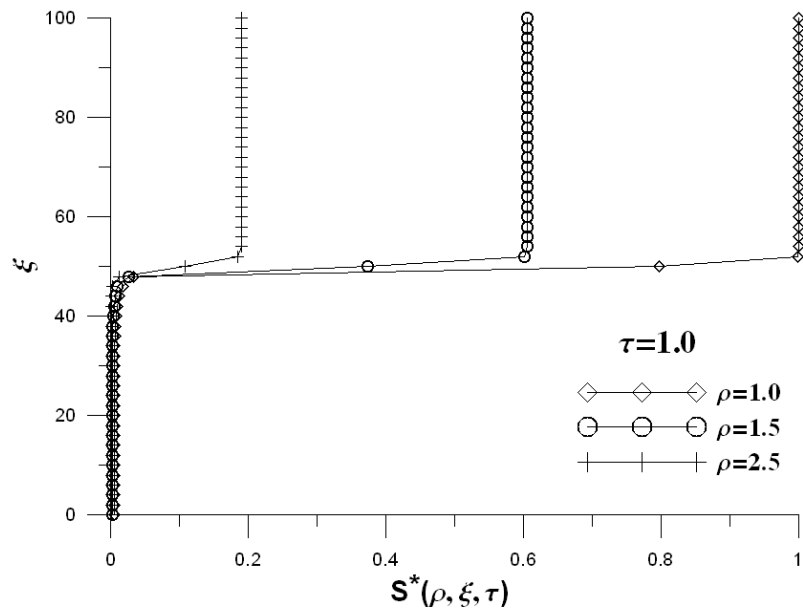


Figure 3a The drawdown distribution at dimensionless time for various ρ

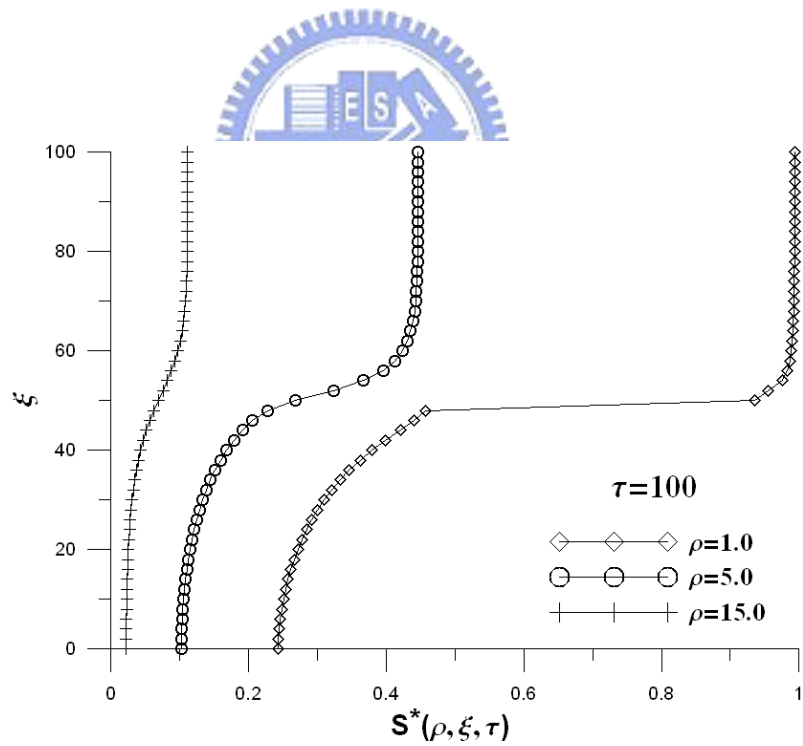


Figure 3b The drawdown distribution at dimensionless time $\tau = 100$ for various ρ

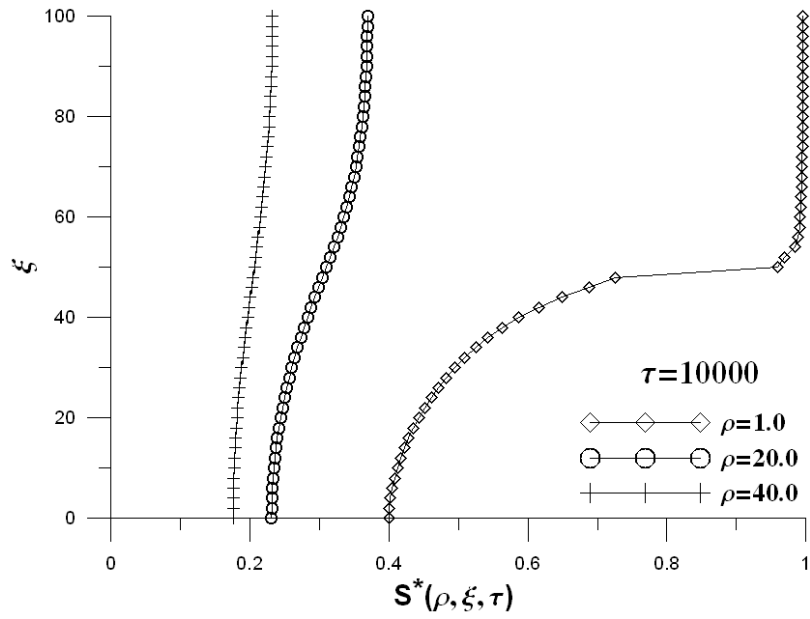


Figure 3c The drawdown distribution at dimensionless time $\tau = 10^4$ for various ρ

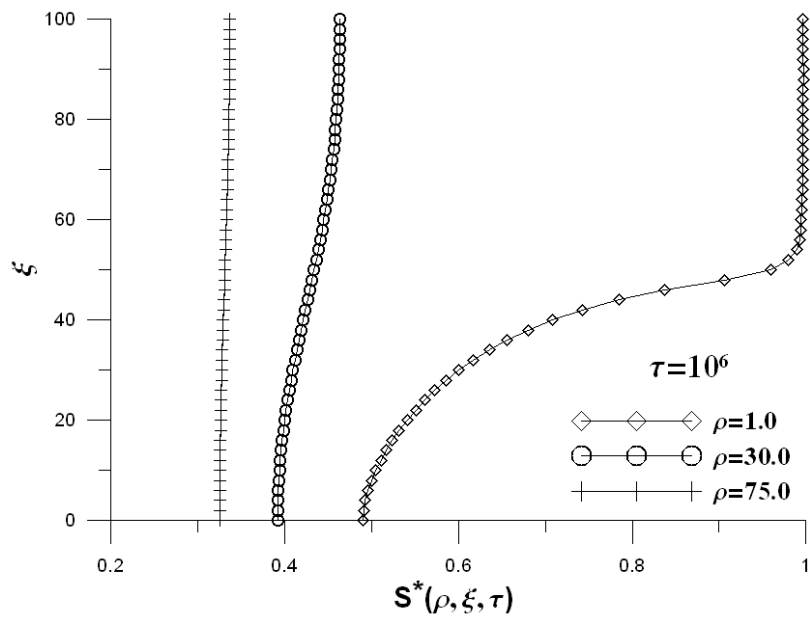


Figure 3d The drawdown distribution at dimensionless time $\tau = 10^6$ for various ρ

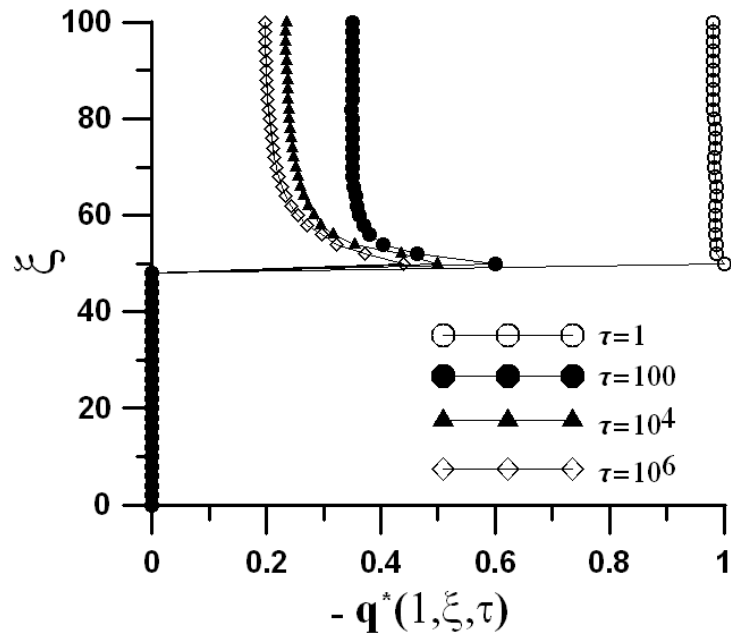


Figure 4 The distribution of flux along the well screen at different dimensionless time



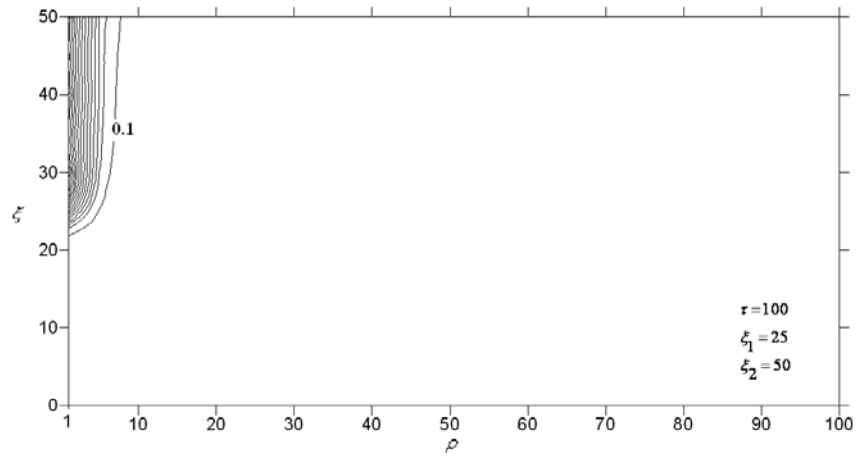


Figure 5(a) The spatial drawdown contours at dimensionless time $\tau = 100$

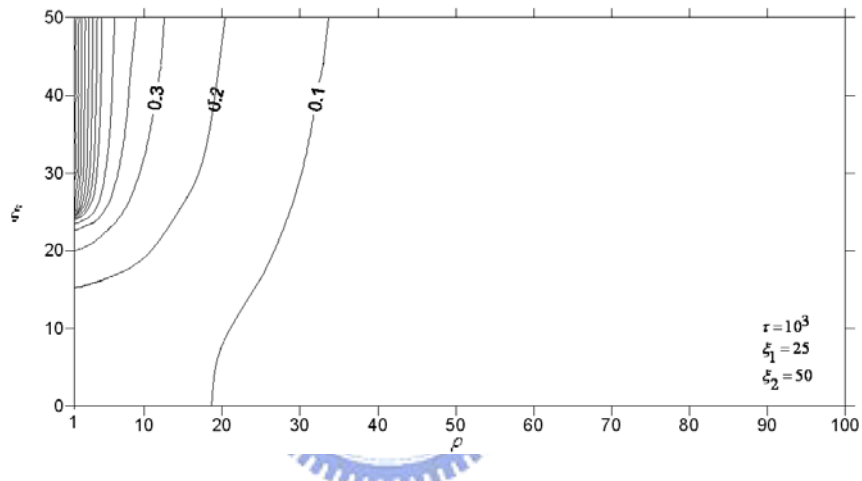


Figure 5(b) The spatial drawdown contours at dimensionless time $\tau = 10^3$

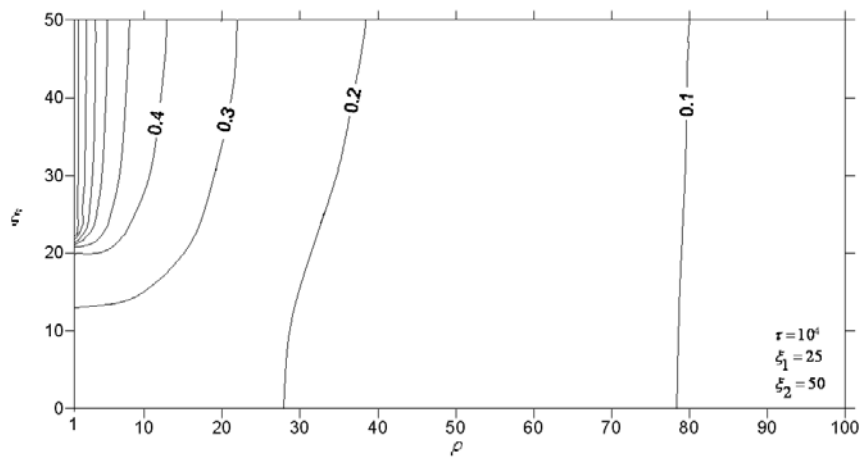


Figure 5(c) The spatial drawdown contours at dimensionless time $\tau = 10^4$

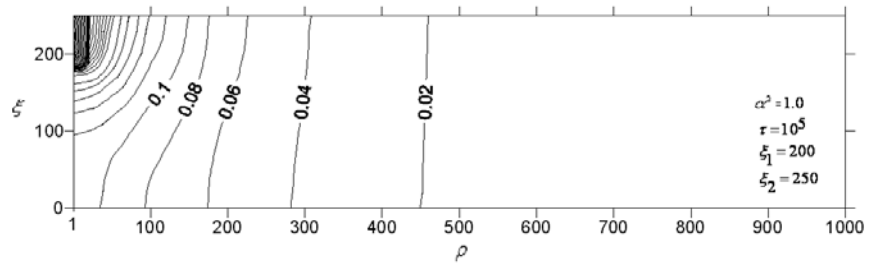


Figure 6(a) The spatial drawdown contours at dimensionless time $\tau = 10^5$ for $\alpha^2 = 1.0$

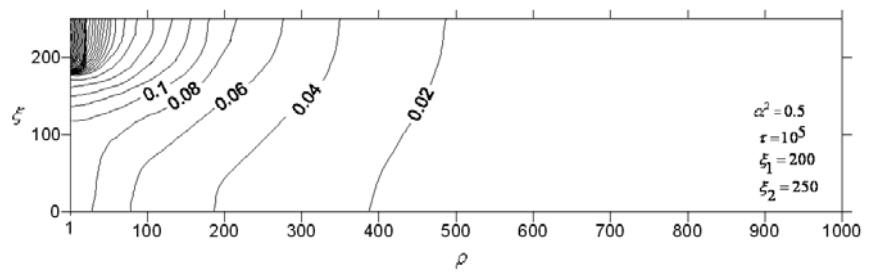


Figure 6(b) The spatial drawdown contours at dimensionless time $\tau = 10^5$ for $\alpha^2 = 0.5$



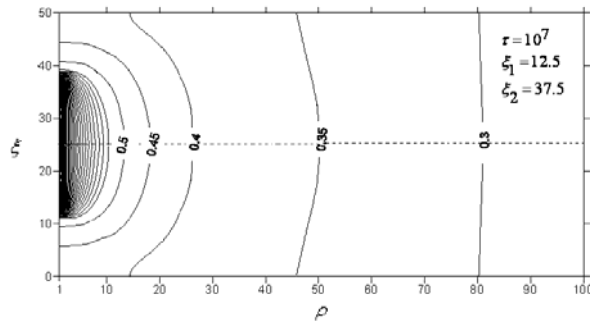


Figure 7(a) The spatial drawdown contours at dimensionless time $\tau = 10^6$ for $\xi_1 = 12.5$ and $\xi_2 = 37.5$ with $\beta = 50$

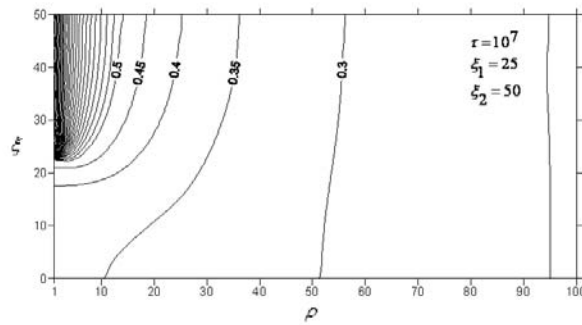
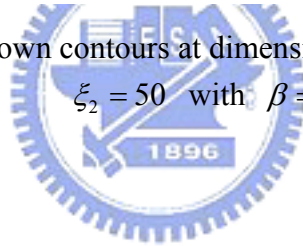


Figure 7(b) The spatial drawdown contours at dimensionless time $\tau = 10^6$ for $\xi_1 = 25$ and $\xi_2 = 50$ with $\beta = 50$



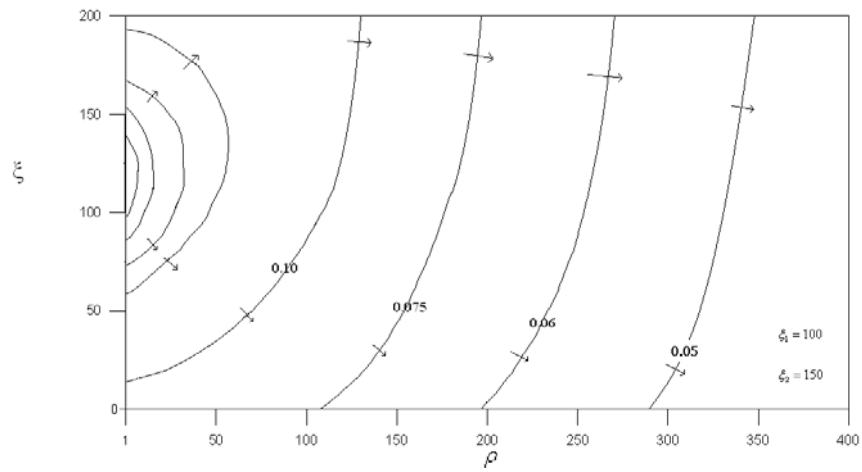


Figure 8 The spatial drawdown contours as at dimensionless time $\tau = 10^7$ for $\xi_1 = 100$ and $\xi_2 = 150$



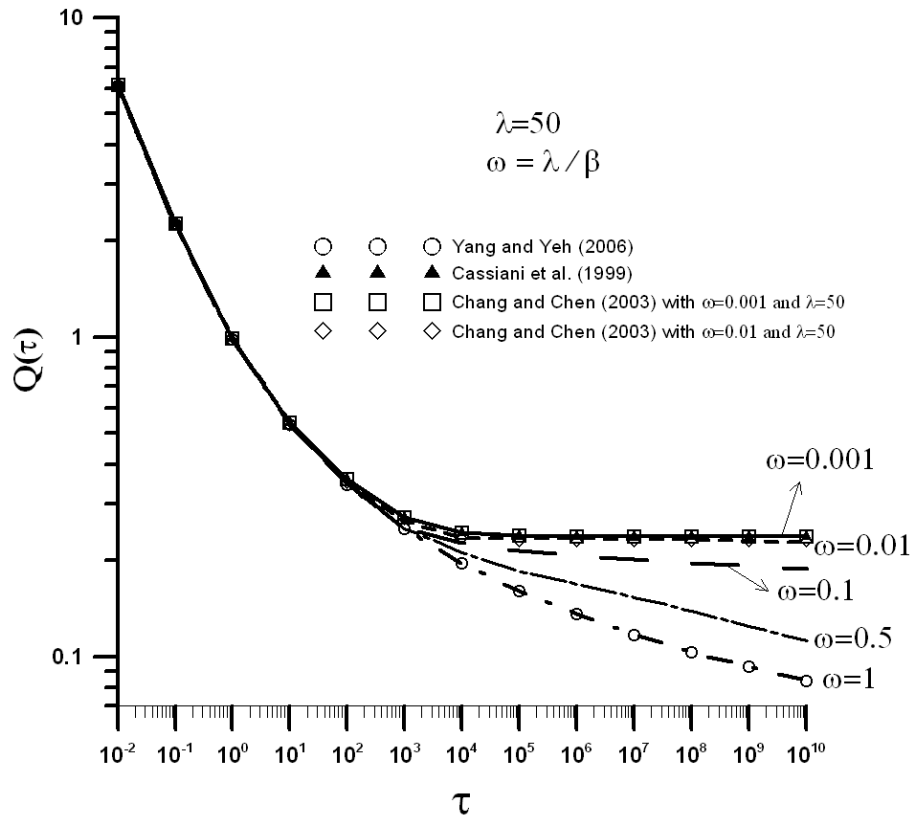


Figure 9 The influence of the penetration ratio on the flux



VITA (個人簡歷)

姓 名	張雅琪
性 別	女
生 日	民國 69 年 03 月 14 日
學 經 歷	1998-2002 學士，交通大學土木工程學系
	2002-2003 交通大學環境工程研究所碩士班
	2003-2009 交通大學環境工程研究所博士班
	2007-2008 Visiting Scholar, Environmental Science and Engineering, University of North Carolina, USA
行動電話	0988314404
通訊電話	03-5712121#55527
通訊地址	300 新竹市交通大學環境工程研究所
E-mail	rachel.ev91g@nctu.edu.tw

PUBLICATION LIST

(A) Journal Papers

1. Yeh, H. D., and Y. C. Chang, 2006, New Analytical Solutions for Groundwater Flow in Wedge-shaped Aquifers with Various Topographic Boundary Conditions, Vol. 29, No. 3, 471-480, *Advances in Water Resources*. (SCI)
2. Y. C. Chang and H. D. Yeh, 2007, Optimum Allocation for Soil Contamination Investigations in Hsinchu, Taiwan by Double Sampling, *Soil Science Society of America Journal*, 71(5), 1585-1592, doi: 10.1061/sssaj1006.0130. (SCI)
3. Y. C. Chang, H. D. Yeh and Y. C. Hung, 2008, Determination of the parameter pattern and values for a one-dimensional multi-zone unconfined aquifer, *Hydrogeology Journal*, 16, 205-214. doi :10.1007/s10040-007-0228-3 (SCI)
4. Y. C. Chang and H. D. Yeh, 2007, Analytical solution for groundwater flow in an anisotropic sloping aquifer with arbitrarily located multiwells, *Journal of Hydrology*, 347, 143-152, 10.1016/j.jhdrol.2007.09.012. (SCI)
5. H. D. Yeh, Y. C. Chang and V. A. Zlotnik, 2008, Stream Depletion in Wedge-Shaped Aquifers, *Journal of Hydrology*, 349, 501-511. (SCI)
6. H. D. Yeh, S. B. Wen, Y. C. Chang and C. S. Lu, 2008, A new approximate solution for chlorine decay in pipes, *Water Research*, 42, 2787-2795. (SCI)
7. Chang, Y. C., H. D. Yeh, 2009, New solutions to the constant-head test performed at a partially penetrating well. *Journal of Hydrology*, doi:10.1016/j.jhydrol.2009.02.016 (SCI; IF:2.161)
8. Chang, Y. C., H. D. Yeh, 2009, Solutions for mixed boundary value problem in a constant-head test aquifer. *Water Resources Research* (In review)
9. Chang, Y. C., H. D. Yeh, K. F. Liang and M. C. T. Kuo, 2009, Scale dependency of fractional flow dimension in a fractured formation, *Journal of Hydrology* (In preparation)

10. Chang, Y. C., H. D. Yeh, Solutions for radial two-zone flow in unconfined aquifer under constant-head test. (In preparation)
11. Chang, Y. C., H. D. Yeh, G. Y. Chen, The flow rate across the wellbore in a two-zone unconfined aquifer. (In preparation)

(B) Conference papers

1. 張雅琪、葉弘德，92 年 4 月，離群值的檢定—以新竹市土壤污染數據為對象，第四屆環境管理研討會，嘉義，台灣，論文集光碟版 2002.
2. 張雅琪、葉弘德，92 年 11 月，使用雙重採樣法決定最佳採樣樣本數—以新竹市土壤污染數據為對象，環工學會第十五屆年會及第一屆土壤與地下水技術研討會，國立中興大學，台中，論文摘要集頁，論文集光碟版。
3. 張雅琪、葉弘德，楔形含水層在定水頭邊界條件下之解析解，第 14 屆水利工程研討會，新竹，台灣，2004.
4. 張雅琪、葉弘德，93 年 10 月，水平多層自由含水層之地下水流研析，九十三年度農業工程研討會，中國農業工程學會，桃園，論文摘要集 245 頁，論文集光碟版 1523-1529 頁。
5. Yeh, H. D., Y. C. Chang, and Y. C. Huang, 2005, Identifying horizontal multi-zone unconfined aquifer parameters using simulated annealing, AOGS 2nd annual meeting, Singapore, 58-HS-A0504.
6. 張雅琪、葉弘德，94 年月，應用多變量統計分析近海工業區之地下水污染，第九屆土壤與地下水污染整治研討會，台北，論文集 203~214 頁。
7. 張雅琪、葉弘德，94 年 9 月，楔形含水層在不同邊界條件下之地下水流研析，九十四年電子計算機於土木水利工程應用研討會，中國土木水利工程學會，國立成功大學，台南，論文集(III)491-496 頁。
8. 張雅琪、葉弘德，94 年 11 月，應用多變量統計分析地下水污染源:以台灣南部某污染場址為案例，九十四年度農業工程研討會，中國農業工程學會，桃園，論文摘要集 111 頁，論文集光碟版。

9. 張雅琪、葉弘德，94 年 11 月，利用統計方法區分地下水污染降解模式，第三屆土壤與地下水研討會，環境工程學會，桃園，論文摘要集 487 頁。
10. Chang, Y. C., and H. D. Yeh, 2006, Analytical Solution for Anisotropic Sloping Aquifers with Arbitrarily Located Multiwells and Transient Recharge, AGU Western Pacific Meeting, Beijing, China, H41D-0084, WP96.
11. 張雅琪、葉弘德、梁康阜、郭明錦、范愷軍，95 年 10 月，破碎帶含水層流場的流動幾何形狀及水力特性之檢定，九十五年農業工程研討會，中國農業工程學會，國立成功大學，台南市，論文集 98-99 頁，論文集光碟版 331.PDF
12. 張雅琪、葉弘德，96 年 8 月，計算楔形含水層的河川消耗速率及體積，第十六屆水利工程研討會，中國土木水利工程學會，國立聯合大學理工學院，苗栗，論文摘要集 100 頁，論文集檔案 PDF：542-548。

